

# CONSTRAINING THE QUADRUPOLE MOMENT OF STELLAR-MASS BLACK-HOLE CANDIDATES WITH THE CONTINUUM FITTING METHOD

COSIMO BAMBI

Institute for the Physics and Mathematics of the Universe, The University of Tokyo  
Kashiwa, Chiba 277-8583, Japan

ENRICO BARAUSSE

Department of Physics, University of Maryland  
College Park, Maryland 20742, United States

(Dated: August 17, 2021)  
Draft version August 17, 2021

## ABSTRACT

Black holes in General Relativity are known as Kerr black holes and are characterized solely by two parameters, the mass  $M$  and the spin  $J$ . All the higher multipole moments of the gravitational field are functions of these two parameters. For instance, the quadrupole moment is  $Q = -J^2/M$ , which implies that a measurement of  $M$ ,  $J$ , and  $Q$  for black hole candidates would allow one to test whether these objects are really black holes as described by General Relativity. While future gravitational-wave experiments will be able to test the Kerr nature of these objects with very high accuracy, in this paper we show that it is possible to put constraints on the quadrupole moment of stellar-mass black hole candidates by using presently available X-ray data of the thermal spectrum of their accretion disk.

*Subject headings:* accretion, accretion disks — black hole physics — general relativity — X-rays: binaries

## 1. INTRODUCTION

The most general stationary and axisymmetric black-hole (BH) solution of Einstein’s equations in a four-dimensional, asymptotically flat spacetime is given by the Kerr geometry (Kerr 1963). Today there are at least two classes of astrophysical BH candidates: stellar-mass objects in X-ray binary systems (mass  $M \sim 5 - 20 M_{\odot}$ ) (Cowley 1992; Remillard & McClintock 2006) and super-massive objects at the center of most galaxies ( $M \sim 10^5 - 10^{10} M_{\odot}$ ) (Kormendy & Richstone 1995). The existence of a third class of objects, intermediate-mass BHs with  $M \sim 10^2 - 10^4 M_{\odot}$  (Miller & Colbert 2004), is still controversial because their detections are indirect and definitive dynamical measurements of their masses are still lacking (Miller & Colbert 2004).

All these objects are supposed to be Kerr BHs because they cannot be explained otherwise without introducing new physics. In particular, stellar-mass BH candidates in X-ray binary systems are too heavy to be neutron or quark stars for any reasonable matter equation of state (Rhoades & Ruffini 1974; Kalogera & Baym 1996). Observations of stellar orbits around the super-massive BH candidate Sgr A\* at the center of the Galaxy show that this object is too massive, compact, and old to be a cluster of non-luminous bodies (Maoz 1998) or a fermion ball (Schödel et al. 2002) (*i.e.*, an object made of sterile neutrinos, gravitinos or axinos supported by degeneracy pressure (Tsiklauri & Viollier 1998)). Other exotic alternatives such as boson stars (Torres et al. 2000) and gravastars (Mazur & Mottola 2004; Chirenti & Rezzolla 2007, 2008) seem to be disfavored by the near-infrared observations of Sgr A\* (Broderick & Narayan 2006; Broderick et al. 2009).

In spite of this body of indirect evidence, a definitive proof that BH candidates are really described by the Kerr solution of General Relativity is still elusive. A framework within which to test the Kerr BH hypothesis was first put forward by Ryan (1995, 1997a,b), who considered a general stationary, axisymmetric, asymptotically flat, vacuum spacetime. Such a generic spacetime can be used to describe the gravitational field around a central object, whatever its nature, and its metric can be expressed in terms of the mass moments  $M_{\ell}$  and current moments  $S_{\ell}$  (Geroch 1970; Hansen 1974). Assuming reflection symmetry, the odd  $M$ -moments and even  $S$ -moments are identically zero, so that the non-vanishing moments are the mass  $M_0 = M$ , the mass quadrupole  $M_2 = Q$  and the higher-order even terms  $M_4, M_6, \dots$ , as well as the angular momentum  $S_1 = J$ , the current octupole  $S_3$  and the higher-order odd terms  $S_5, S_7, \dots$ . In the case of a Kerr BH, all the moments  $M_{\ell}$  and  $S_{\ell}$  are locked to the mass and angular momentum by the following relation:

$$M_{\ell} + iS_{\ell} = M \left( i \frac{J}{M} \right)^{\ell} . \quad (1)$$

This is the celebrated “no-hair” theorem (Carter 1971; Robinson 1975; Chruściel & Lopes Costa 2008): an (uncharged) stationary BH is uniquely characterized by its mass and spin angular momentum. Therefore, a measurement of the

mass, spin and higher moments (starting with the quadrupole moment  $Q$ ) of BH candidates would permit testing Eq. (1) and therefore the Kerr-nature of these objects.

Ryan’s idea was to use future gravitational-wave observations of extreme-mass ratio inspirals (EMRIs, *i.e.*, systems consisting of a stellar-mass BH orbiting a super-massive BH in a galactic center) to perform this test. EMRIs will be a key source for the future-space based detector LISA: because the stellar-mass BH will orbit the super-massive BH  $\sim 10^6$  times during LISA’s lifetime, slowly spiralling in due to the emission of energy and angular momentum via gravitational waves, even a small deviation from the Kerr geometry will build up an observable dephasing in the gravitational waveforms, thus allowing one to map the spacetime of super-massive BHs with very high accuracy. Ryan’s spacetime mapping idea originated a whole line of research aiming at using LISA’s observations of EMRIs to test the Kerr nature of super-massive BHs (Collins & Hughes 2004; Vigeland & Hughes 2010; Apostolatos et al. 2009; Lukes-Gerakopoulos et al. 2010; Glampedakis & Babak 2006; Gair et al. 2008; Kesden et al. 2005; Barausse et al. 2007; Barausse & Rezzolla 2008; Barack & Cutler 2007) and even General Relativity itself (Sopuerta & Yunes 2009; Barausse & Sotiriou 2008). Another independent (and complementary) test of the no-hair theorem with LISA uses BH quasi-normal modes (Berti et al. 2009). Because the frequencies of these modes encode the multipolar structure (1) of the Kerr geometry, they can be used to test consistency with the Kerr solution and to distinguish it from boson stars (Berti & Cardoso 2006) or gravastars (Chirenti & Rezzolla 2007).

Besides these tests based on gravitational waves, there are other proposals using electromagnetic radiation. Constraints on the quadrupole moment of the compact companion of radio pulsars can be obtained with timing measurements (Wex & Kopeikin 1999). Astrometric monitoring of stars orbiting at milliparsec distances from Sgr A\* may be used to test the no-hair theorem for the super-massive BH candidate at the center of the Galaxy (Will 2008; Merritt et al. 2010). A very promising way to measure deviations from the Kerr metric is represented by future observations of the “shadow” of super-massive BH candidates through very long baseline interferometry (VLBI) experiments (Bambi & Yoshida 2010a; Johannsen & Psaltis 2010a,b). The study of quasi-periodic variability in BH spectra may also test the geometry of the spacetime around BH candidates (Johannsen & Psaltis 2010c). Remarkably, Psaltis & Johannsen (2010d) also shows that the data for iron  $K\alpha$  emission lines in thin accretion disks can *already* constrain deviations from the Kerr geometry. Although these measurements yield much less accurate constraints than what will be achieved with LISA, and can be subject to critiques (see Titarchuk et al. (2009), who show that iron- $K\alpha$  lines with the same features as those attributed to BH candidates are observed also around white dwarfs), these data are available *now*, which is not the case for all the other tests reviewed above. However, because of the controversial interpretation of the origin of these lines, and because Psaltis & Johannsen (2010d) finds a degeneracy between the spacetime’s quadrupole and spin (*i.e.*, similar shapes for the iron- $K\alpha$  lines can be obtained with a Kerr BH or with a non-Kerr object with spin and quadrupole slightly shifted from the Kerr values), it is important to explore other techniques to test the no-hair theorem with *present* data.

In this paper we propose using the continuum spectrum of BH candidates, which has been shown to be potentially a promising tool to tell Kerr BHs from specific alternatives such as gravastars (Harko et al. 2009a), BHs in Chern-Simons gravity (Harko et al. 2010b), BHs in Horava-Lifschitz gravity (Harko et al. 2010a) or certain classes of naked singularities (Harko et al. 2009b; Takahashi & Harada 2010; Kovacs & Harko 2010). While these attempts highlighted some important differences between the spectra of these objects and those of Kerr BHs, they relied on specific models for the BH candidate, and did not investigate whether presently available data allow one to break the degeneracy mentioned above between the parameters of these objects and those of a Kerr BH (*i.e.*, whether present X-ray data can tell the spectrum of a non-Kerr object from that of a Kerr BH with arbitrary  $J$  and  $M$ ). In this paper we address both issues, (*i*) by considering a very general model for the BH candidate (*i.e.*, one which allows its quadrupole moment to slightly deviate from the Kerr value, thus approximately describing a variety of almost-Kerr objects), (*ii*) by comparing our model to present X-ray data, although in a simplified way, and (*iii*) by discussing the sources of systematic error that might affect the data and that must be properly understood before one can perform robust tests of the no-hair theorem.

In the range 0.1 keV – 1 MeV, the generic spectrum of a stellar-mass BH candidate is characterized by three components, even if their relative intensities vary with the object and, for a given object, with time: *i*) a soft X-ray component (energies < 10 keV), *ii*) a hard power law X-ray component with an exponential cutoff (energies in the range 10 – 200 keV, photon spectral index in the range 1 – 2.5), and *iii*) a  $\gamma$ -ray component (energies > 300 keV). For a review, see e.g. Liang (1998). The soft X-ray component is commonly interpreted as the thermal spectrum of a thin disk, while the exact origin of the other two components is not so clear.

Geometrically thin and optically thick accretion disks can be described by the Novikov-Thorne model (Novikov & Thorne 1973). They are expected when the accretion flow is radiatively efficient, which requires a luminosity  $L \lesssim 0.3 L_{Edd}$ , where  $L_{Edd}$  is the Eddington limit. The emission is blackbody-like. Assuming that the inner edge of the disk is at the innermost stable circular orbit (ISCO)<sup>1</sup>, the disk luminosity of a Kerr BH is determined only by its mass,  $M$ , the mass accretion rate,  $\dot{M}$ , and the spin parameter,  $a = J/M^2$ . This fact can thus be exploited to estimate the spin of stellar-mass BH candidates (Zhang et al. 1997). This is the continuum fitting method and at present has been used to estimate the spin parameter of a few stellar-mass BH candidates (McClintock et al. 2010)<sup>2</sup>. Basically, knowing the mass of the object, its distance from us, and the inclination angle of the disk, it is possible to fit the soft

<sup>1</sup> Such an assumption is supported either by observational facts (Steiner et al. 2010a) and numerical simulations (Shafee et al. 2008; Penna et al. 2010) (but see Noble et al. (2010)).

<sup>2</sup> For super-massive BHs, the disk temperature is lower (the effective temperature scales like  $M^{-0.25}$ ) and this approach cannot be applied.

X-ray component of the source and deduce  $a$  and  $\dot{M}$ .

In this paper, we compute the thermal spectrum of a geometrically thin and optically thick accretion disk around a generic compact object. We use a subclass of Manko-Novikov spacetimes (Manko & Novikov 1992), which are stationary, axisymmetric, and asymptotically flat exact solutions of the vacuum Einstein equations. In addition to the mass and the spin of the massive object, here we have the anomalous quadrupole moment,  $q$ . The latter measures the deformation of the massive object with respect to a Kerr BH: when  $q > 0$ , the object is more oblate than a Kerr BH, when  $q < 0$ , it is more prolate, while, for  $q = 0$ , we recover the Kerr metric. The value of  $q$  determines the radius of the ISCO and changes the high frequency region of the spectrum of the disk.

In general, this makes the spectrum of the disk almost degenerate in  $a$  and  $q$ . However, only in the Kerr case the radius of the ISCO goes to  $M$  as  $a$  approaches 1. For  $q \neq 0$ , even a small deviation from the Kerr metric makes the radius of the ISCO significantly larger than  $M$ . Since current X-ray observations suggest that there are objects with small ISCO radius, one can in principle obtain interesting constraints on the value of  $q$ .

The purpose of this paper is therefore to present a preliminary investigation, showing that X-ray continuum spectra can potentially be used to constraint small quadrupole deviations away from the Kerr metric, once all the physical effects have been included in the model and all systematics have been understood. In particular, our computation of the disk's spectrum does not include the effect of light bending. This is a simplification of our model and there are no reasons for the light bending to be negligible with respect to the other relativistic effects (Doppler boosting, gravitational redshift, and frame dragging). Another subtle issue is the computation of the spectral hardening factor (here not discussed), which is another weak point of our approach. Our study has to be taken as a preliminary investigation and significant work has still to be done before the continuum fitting method can be used to obtain reliable constraints on the Kerr geometry around stellar-mass BH candidates.

The content of this paper is as follows. In Sec. 2, we review the basic properties of a geometrically thin and optically thick accretion disk and how to compute its spectrum. In Sec. 3 and 4, we present the results of our calculations, respectively for a Kerr BH and for a generic object with  $q \neq 0$ . In Sec. 5, we show how current observations can be used to constrain  $q$ , while in Sec. 6 we discuss the possible systematic errors that could affect the continuum fitting technique and therefore our analysis. Lastly, in 7 we report our conclusions. The Manko-Novikov spacetime is reviewed in Appendix A, and the properties of its ISCO are discussed in Appendix B.

Throughout the paper we use units in which  $G_N = c = 1$ , unless stated otherwise.

## 2. THERMAL SPECTRUM OF A THIN DISK

The standard model for a geometrically thin and optically thick accretion disk is due to Novikov and Thorne (Novikov & Thorne 1973). In a generic stationary, axisymmetric and asymptotically flat spacetime, one assumes that the disk is on the equatorial plane, that the disk's gas moves on nearly geodesic circular orbits, and that the radial heat transport is negligible compared to the energy radiated from the disk's surface. From the conservation laws for the rest-mass, angular momentum and energy, one can deduce three basic equations for the time-averaged radial structure of the disk (Page & Thorne 1974). These equations determine the radius-independent time-averaged mass accretion rate  $\dot{M}$ , the time-averaged energy flux  $\mathcal{F}(r)$  from the surface of the disk (as measured by an observer comoving with the disk's gas) and the time-average torque  $W_\phi^r(r)$ :

$$\dot{M} = -2\pi\sqrt{-G}\Sigma u^r = \text{const.} \quad (2)$$

$$\mathcal{F}(r) = \frac{\dot{M}}{4\pi\sqrt{-G}}f(r), \quad (3)$$

$$W_\phi^r(r) = \frac{\dot{M}}{2\pi\sqrt{-G}}\frac{\Omega L_z - E}{\partial_r\Omega}f(r). \quad (4)$$

Here  $\Sigma$  is the surface density,  $u^r$  is the radial 4-velocity,  $G$  is the determinant of the near equatorial plane metric in cylindrical coordinates<sup>3</sup>,  $E$ ,  $L_z$ , and  $\Omega$  are respectively the conserved specific energy, the conserved  $z$ -component of the specific angular momentum, and the angular velocity  $d\phi/dt$  for equatorial circular geodesics, and  $f(r)$  is given by

$$f(r) = \frac{-\partial_r\Omega}{(E - \Omega L_z)^2} \int_{r_{\text{in}}}^r (E - \Omega L_z) (\partial_r L_z) d\rho, \quad (5)$$

where  $r_{\text{in}}$  is the inner radius of the accretion disk and is assumed to be the ISCO radius. More details are given in Appendix B.

Since the disk is in thermal equilibrium, the emission is blackbody-like and we can define an effective temperature  $T = T(r)$  from the relation  $\mathcal{F} = \sigma T^4$ , where  $\sigma = 5.67 \times 10^{-5} \text{ erg s}^{-1} \text{ cm}^2 \text{ K}^{-4}$  is the Stefan-Boltzmann constant. Neglecting the effect of light bending, the *equivalent isotropic luminosity* is

$$L(\nu) = \frac{8\pi h}{c^2} \cos i \int_{r_{\text{in}}}^{r_{\text{out}}} \int_0^{2\pi} g^3 \frac{\nu_e^3 \sqrt{-G} dr d\phi}{\exp[h\nu_e/(kT)] - 1}, \quad (6)$$

where we have written explicitly the Planck constant  $h$ , the speed of light  $c$ , and the Boltzmann constant  $k$ . Here,

<sup>3</sup>  $\sqrt{-G} = \sqrt{\alpha^2 g_{rr} g_{\phi\phi}}$ , where  $\alpha$  is the lapse function. In Kerr spacetime in Boyer-Lindquist coordinates,  $\sqrt{-G} = r$ .

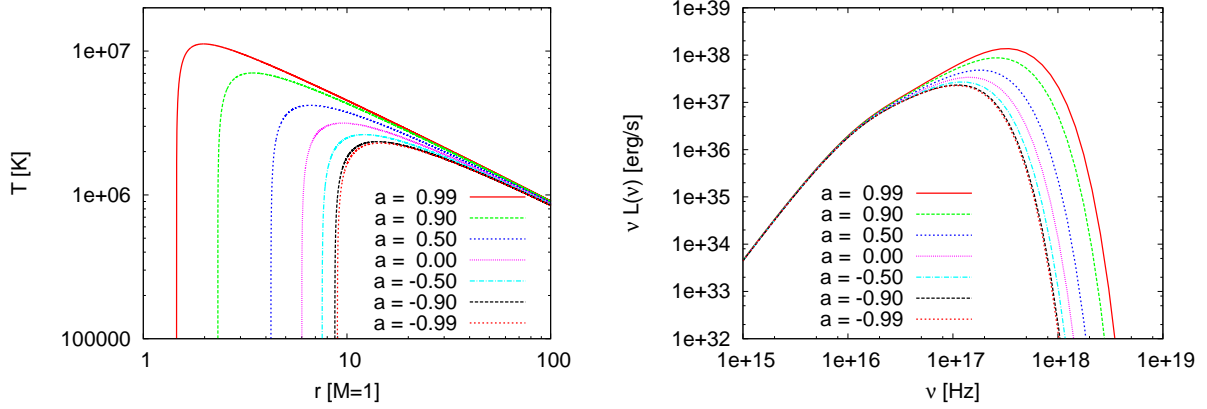


FIG. 1.— Radial profile of the effective temperature (left panel) and spectrum  $\nu L(\nu)$  (right panel) of a thin accretion disk in Kerr spacetime for different value of the spin parameter  $a$ . Here we take the mass  $M = 10 M_{\odot}$ , the mass accretion rate  $\dot{M} = 10^{18}$  g/s, and the inclination angle  $i = 45^{\circ}$ .

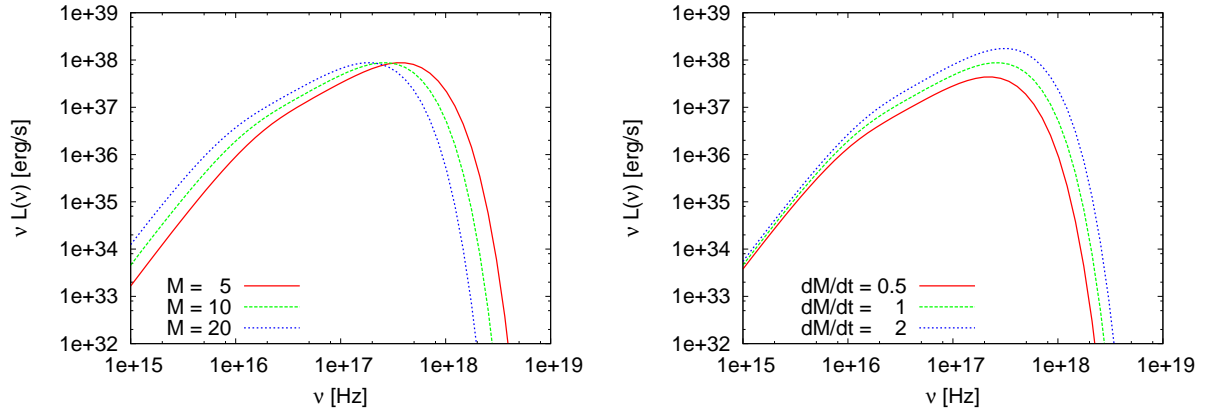


FIG. 2.— Spectrum  $\nu L(\nu)$  of a thin accretion disk in Kerr spacetime with  $a = 0.9$  and an observer inclination angle  $i = 45^{\circ}$ . Left panel: mass  $M = 5, 10, 15 M_{\odot}$  and mass accretion rate  $\dot{M} = 10^{18}$  g/s. Right panel: mass  $M = 10 M_{\odot}$  and mass accretion rate  $\dot{M} = 0.5 \times 10^{18}$  g/s,  $10^{18}$  g/s, and  $2 \times 10^{18}$  g/s.

$i$  is the angle between the distant observer's line of sight and the direction orthogonal to the disk,  $r_{\text{in}}$  and  $r_{\text{out}}$  are respectively the inner and outer radius of the disk, while  $\nu$  is the radiation frequency in the local rest frame of the distant observer and  $\nu_e$  is the frequency in the local rest frame of the emitter. These two frequencies are related by the redshift factor

$$g = \frac{\nu}{\nu_e} = \frac{k_{\mu} u_o^{\mu}}{k_{\mu} u_e^{\mu}}, \quad (7)$$

where  $u_o^{\mu} = (1, 0, 0, 0)$  is the 4-velocity of the observer and  $u_e^{\mu} = (u_e^t, 0, 0, \Omega u_e^t)$  is the 4-velocity of the emitter. Using the normalization condition  $g_{\mu\nu} u_e^{\mu} u_e^{\nu} = -1$ ,  $u_e^t$  can be obtained to be

$$u_e^t = \frac{1}{\sqrt{-g_{tt} - 2g_{t\phi}\Omega - g_{\phi\phi}\Omega^2}}. \quad (8)$$

Because the  $t$ - and  $\phi$ -component of a photon's canonical 4-momentum are conserved quantities in any stationary and axisymmetric spacetime, we can compute the quantity  $k_{\phi}/k_t$  at infinity. The result is  $k_{\phi}/k_t = r \sin \phi \sin i$  and the redshift factor turns out to be

$$g = \frac{\sqrt{-g_{tt} - 2g_{t\phi}\Omega - g_{\phi\phi}\Omega^2}}{1 + \Omega r \sin \phi \sin i}. \quad (9)$$

With  $g$ , we take into account the special and general relativistic effects of Doppler boost, gravitational redshift, and frame dragging.

### 3. SPECTRUM IN KERR SPACETIMES

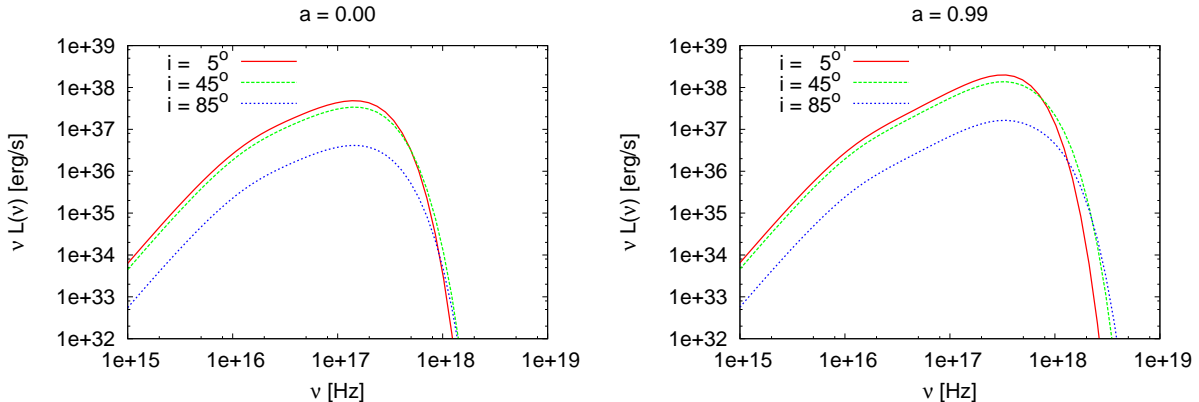


FIG. 3.— Spectrum  $\nu L(\nu)$  of a thin accretion disk in Kerr spacetime with mass  $M = 10 M_{\odot}$  and mass accretion rate  $\dot{M} = 10^{18}$  g/s. Here we consider different observer inclination angles for  $a = 0.00$  (left panel) and  $a = 0.99$  (right panel).

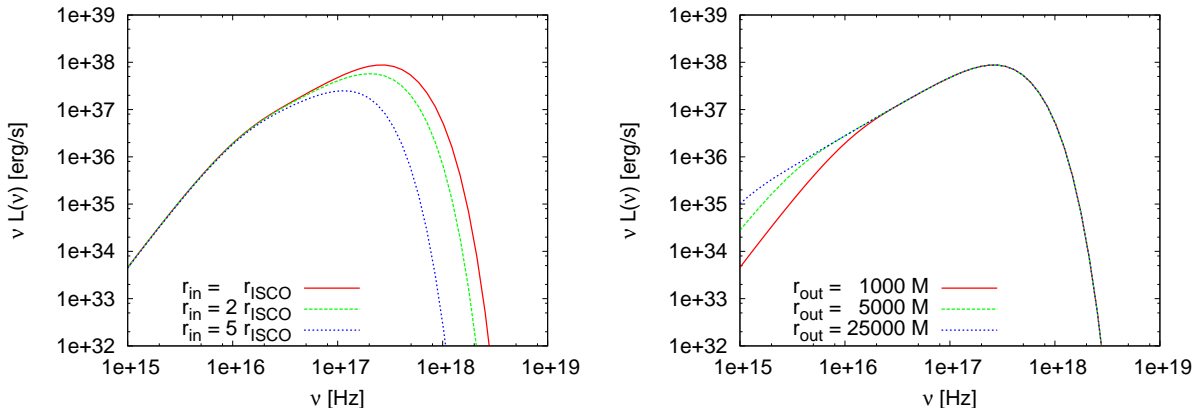


FIG. 4.— Effect of a different inner and outer disk radius. Left panel:  $r_{\text{in}} = r_{\text{ISCO}}$ ,  $r_{\text{in}} = 2 r_{\text{ISCO}}$ , and  $r_{\text{in}} = 5 r_{\text{ISCO}}$ . Right panel:  $r_{\text{out}} = 1000 M$ ,  $r_{\text{out}} = 5000 M$ , and  $r_{\text{out}} = 25000 M$ .

To begin with, we calculate the thermal spectrum of a geometrically thin and optically thick accretion disk around a Kerr BH. Here we have four free parameters determining the luminosity (6): the mass of the BH  $M$ , the spin parameter  $a$ , the mass accretion rate  $\dot{M}$ , and the inclination angle of the disk with respect to the distant observer  $i$ . However, usually  $M$  and  $i$  can be deduced from independent observations (see Section 5 for an example).

The role of the spin parameter is shown in Fig. 1, where we assume  $M = 10 M_{\odot}$ ,  $\dot{M} = 10^{18}$  g/s, and  $i = 45^{\circ}$ . In the left panel, we present the radial profile of the effective temperature and, in the right panel, the observed spectrum  $\nu L(\nu)$ . For  $a < 0$ , we mean that the disk is counterrotating. Since we assume that  $r_{\text{in}} = r_{\text{ISCO}}$ , the spin parameter determines the inner radius of the disk: as  $a$  increases,  $r_{\text{in}}$  decreases and we find warmer matter at smaller radii. At larger radii the effective temperature is essentially independent of the spin parameter. Therefore, a higher spin parameter moves the peak of  $\nu L(\nu)$  to higher frequency and to higher values.

Changing the BH mass while keeping  $\dot{M}$  constant<sup>4</sup> has two effects. For larger masses, the effective temperature decreases ( $T \propto M^{-1/2}$ ) and therefore the peak of spectrum moves to lower frequency. At the same time, the size of the disk increases, increasing the total luminosity. In the left panel of Fig. 2 we show the cases  $M = 5, 10, 15 M_{\odot}$  for  $a = 0.9$ . The role of the mass accretion rate is shown in the right panel of Fig. 2. It is clear that a change in  $\dot{M}$  only changes the effective temperature.

The viewing angle  $i$  determines the effective disk surface seen by the distant observer and the correction due to the Doppler boosting (for  $i = 0^{\circ}$  there is no Doppler boosting)<sup>5</sup>. In Fig. 3 we show the cases  $i = 5^{\circ}, 45^{\circ}$  and  $85^{\circ}$  for  $a = 0$  (left panel) and  $a = 0.99$  (right panel).

Lastly, we show the effect of  $r_{\text{in}}$  and  $r_{\text{out}}$  on the shape of the spectrum. So far we have adopted the standard assumption that the inner radius of the disk is at the ISCO and we have chosen the outer radius  $r_{\text{out}} = 10^3 M$ . However, if  $r_{\text{in}}$  were larger than the radius of the ISCO, it would affect the high frequency part of the spectrum,

<sup>4</sup> While this assumption is useful to single out the effect of a change in  $M$ , if a BH accretes at the Eddington rate one has  $\dot{M} \propto M$ .

<sup>5</sup> We remind the reader that here we neglect the effect of light bending, whose contribution would also depend on the viewing angle.

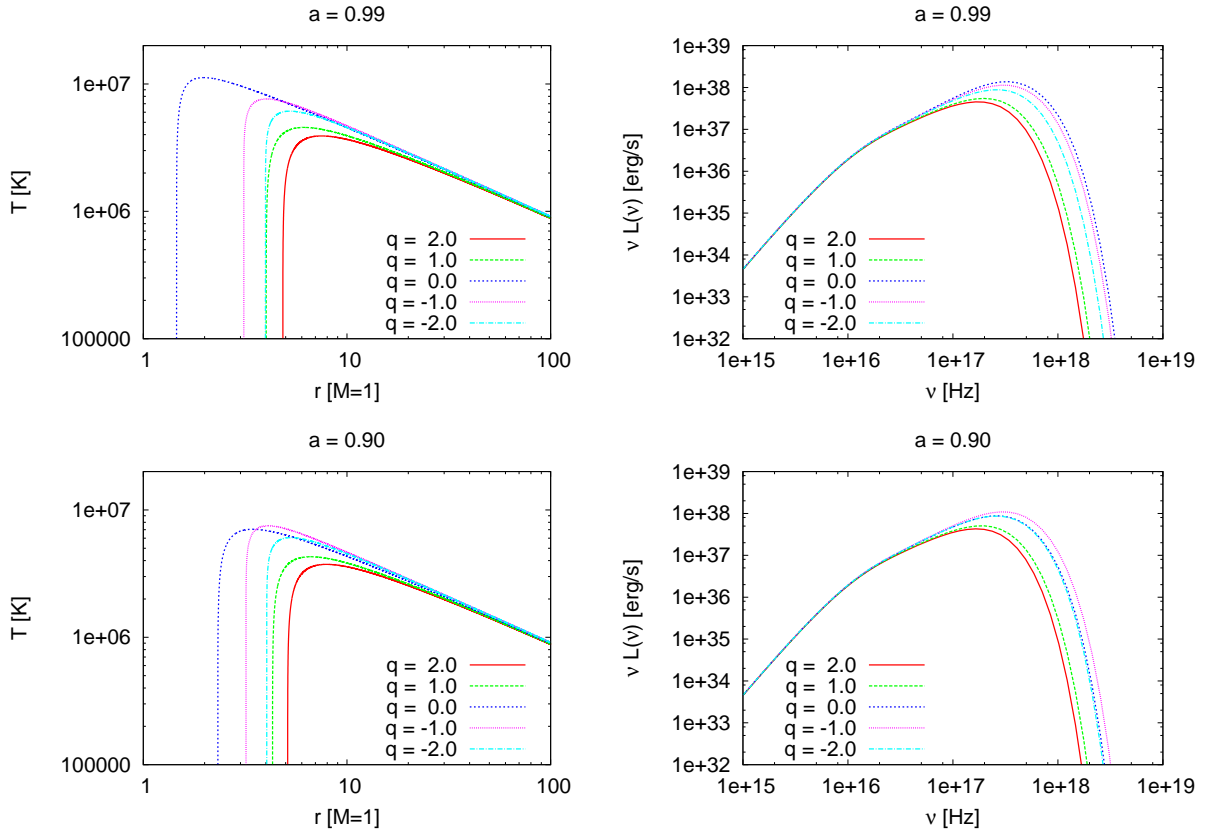


FIG. 5.— Radial profile of the effective temperature (left panels) and spectrum  $\nu L(\nu)$  (right panels) of a thin accretion disk in Manko-Novikov spacetime for spin parameter  $a = 0.99$  (top panels) and  $a = 0.90$  (bottom panels) and for different values of the anomalous quadrupole moment  $q$ . Here we take the mass  $M = 10 M_{\odot}$ , the mass accretion rate  $\dot{M} = 10^{18}$  g/s, and the inclination angle  $i = 45^{\circ}$ .

mimicking a lower spin parameter, see Fig. 4. On the other hand, assuming a larger outer radius of the disk, the spectrum moves the cut-off at lower frequencies, with no changes at higher frequencies.

#### 4. SPECTRUM IN MANKO-NOVIKOV SPACETIMES

Let us now consider the more general case in which the compact object is not a Kerr BH. The gravitational field around a generic compact body can be described by the Manko-Novikov metric, which is a stationary, axisymmetric and asymptotically flat exact solution of the vacuum Einstein equation and has an infinite number of free parameters. The structure of the spacetime presents strong similarities with the  $\delta = 2$  Tomimatsu-Sato spacetime (Tomimatsu & Sato 1972; Kodama & Hikida 2003). Here we restrict our attention to a subclass of the Manko-Novikov solution, where the compact object is determined by its mass  $M$ , its spin parameter  $a = J/M^2$ , and the anomalous quadrupole moment  $q$  which regulates the deviations of the spacetime from the Kerr geometry:

$$q = -\frac{Q - Q_{\text{Kerr}}}{M^3}, \quad (10)$$

where  $Q$  and  $Q_{\text{Kerr}} = -a^2 M^3$  are respectively the quadrupole moment of the object and that of a Kerr BH. In this work, we consider only spin parameters  $|a| \leq 1$ , which is the allowed range in the standard Manko-Novikov solution<sup>6</sup>. As for the value of the anomalous quadrupole moment measuring the deviation from the Kerr metric: for  $q > 0$  the object is more oblate than a Kerr BH; for  $q < 0$  it is more prolate; for  $q = 0$  the Manko-Novikov metric reduces *exactly* to the Kerr metric. Thanks to this property, this subclass of the Manko-Novikov solution, for which we give complete expressions in Appendix A, is a perfect tool to set up a null experiment (Hughes 2006) to test the validity of the Kerr metric and of the no-hair theorem: any experiment pointing at a significantly non-zero value for  $q$  would imply that the compact object under consideration is not a BH as described by General Relativity. This use of the Manko-Novikov metric has been put forward in gravitational-wave astrophysics, namely in Gair et al. (2008). See Collins & Hughes

<sup>6</sup> In the Kerr case,  $|a| \leq 1$  is the condition for the existence of an event horizon. However, in the more general case of a compact object made of some kind of exotic matter, the maximum value of  $|a|$  may in principle be larger than 1 (Bambi & Freese 2009; Bambi et al. 2009, 2010; Bambi & Yoshida 2010b,c). As in the case of the Tomimatsu-Sato family, also the Manko-Novikov solution can probably be extended to describe objects with  $|a| > 1$  (Manko & Moreno 1997). However, if such fast-rotating objects are very compact, they are most likely unstable, at least for small values of  $q$ , due to the ergoregion instability (Pani et al. 2010).

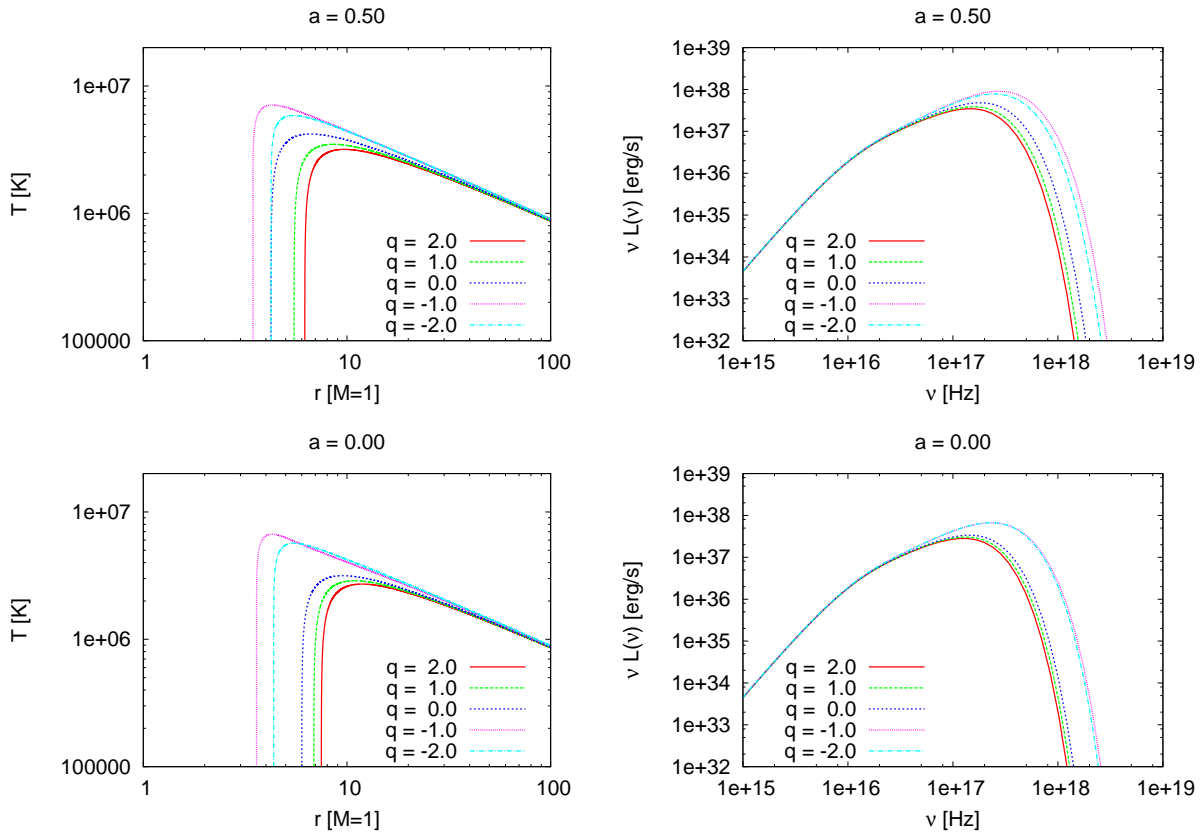


FIG. 6.— As in Fig. 5, for  $a = 0.50$  (top panels) and  $a = 0.00$  (bottom panels).

(2004); Vigeland & Hughes (2010); Glampedakis & Babak (2006) for other metrics which reduce exactly to the Kerr metric when the equivalent of our anomalous quadrupole parameter  $q$  is set to 0, and which can therefore be used to perform null experiments testing the Kerr geometry.<sup>7</sup>

In Figs. 5, 6, and 7, we show the radial profile of the thin accretion disk’s effective temperature and the spectrum  $\nu L(\nu)$  for a few values of  $a$  and  $q$ . We still assume  $M = 10 M_{\odot}$ ,  $\dot{M} = 10^{18}$  g/s, and  $i = 45^{\circ}$ . For a given spin parameter, the value of  $q$  determines the radius of the ISCO – see also Appendix B. Since the temperature of the disk is higher at small radii, a non-zero  $q$  produces corrections in the high frequency region of the spectrum, while at low frequencies there are no changes. The effect is quite small for slow-rotating objects or counterrotating disks, while it becomes relevant, and actually non-negligible, for fast-rotating bodies and corotating disks. There are two reasons for this: a small deviation from  $q \neq 0$  produces a larger variation in the radius of the ISCO for higher spin parameters – see Fig. 9 in Appendix B – and, because the ISCO is closer to the compact object as  $a$  approaches 1, the spectrum of the disk is more sensitive to small deviations in the multipole moment expansion. This is the contrary of what happens in the Tomimatus-Sato spacetimes, where for  $|a| \rightarrow 1$  all the solutions reduce to an extreme Kerr BH and thus deviations from the Kerr metric are more relevant for low spin parameters (Bambi & Yoshida 2010a).

##### 5. OBSERVATIONAL CONSTRAINTS: THE CASE OF M33 X-7

As an example of how accretion-disk thermal spectra can already put significant constraints on the deviation  $q$  of the quadrupole moment of BH candidates from that of a Kerr BH (*cf.* Eq. (10)), we consider the case of M33 X-7. This object is an eclipsing X-ray binary consisting of a BH candidate accreting from a companion star (Pietsch et al. 2006), and its orbital parameters and its distance are measured with the highest accuracy among all known BH binaries (Orosz et al. 2007) (see Table 1). In particular, the BH candidate’s mass is measured to be  $M = 15.65 \pm 1.45 M_{\odot}$ , while the disk’s inclination is  $i = 74.6^{\circ} \pm 1^{\circ}$  and the distance is  $d = 840 \pm 20$  kpc (Orosz et al. 2007).

The accurate knowledge of  $M$ ,  $i$  and  $d$  allows the continuum fitting method (Zhang et al. 1997) to extract reliable information on the spin of the BH candidate. By essentially fitting the Chandra and XMM-Newton spectra of M33 X-7 with a relativistic accretion disk model depending on the spin  $a$ , the Eddington ratio  $\ell = L_{\text{bol}}/L_{\text{Edd}}$  (where  $L_{\text{bol}}$  and

<sup>7</sup> The “bumpy BHs” of Collins & Hughes (2004); Vigeland & Hughes (2010) seem related to the Manko-Novikov general solution because they too allow an arbitrary multipolar structure for the non-Kerr spacetime. The “quasi-Kerr” metric of Glampedakis & Babak (2006), instead, is an (approximate) solution of the vacuum Einstein equations only for small values of the spacetime’s spin, and allows only quadrupolar deformations. For these reasons, bumpy BHs or Manko-Novikov spacetimes are preferable options to test general deviations from the Kerr metric.

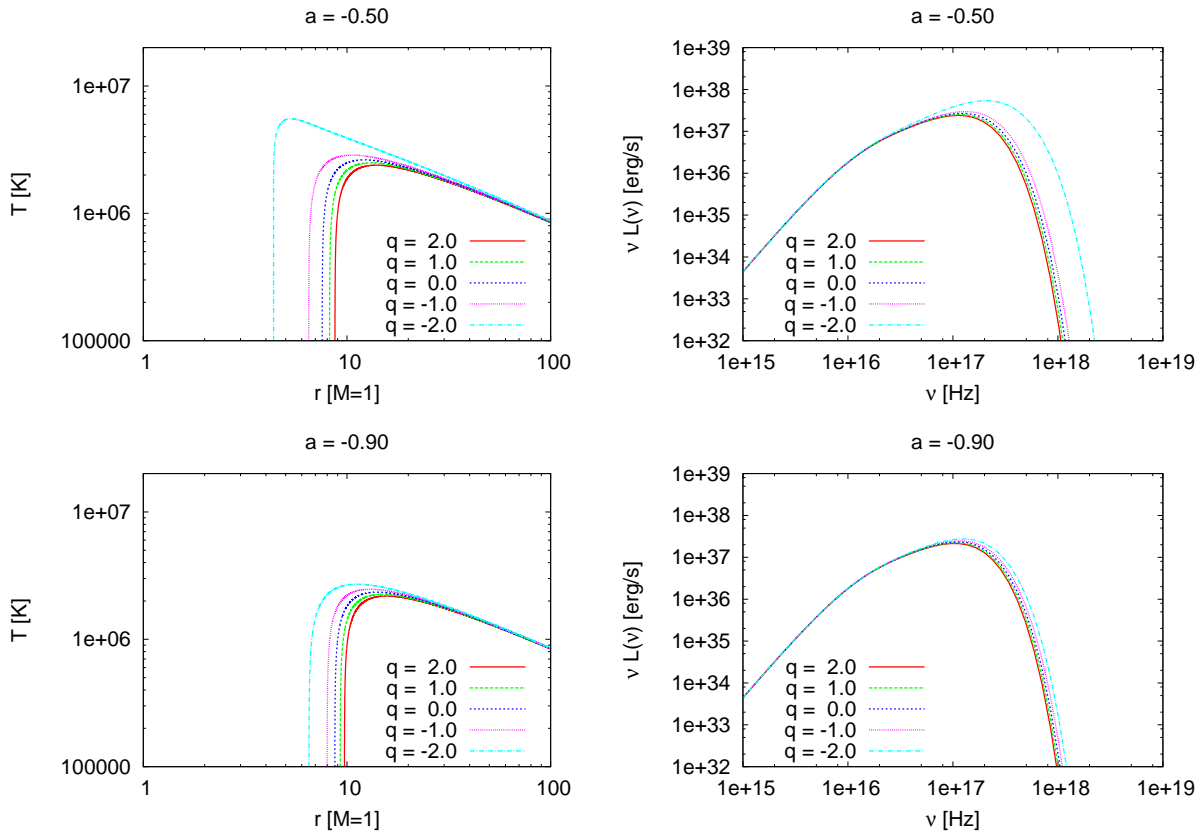


FIG. 7.— As in Fig. 5, for  $a = 0.50$  (top panels) and  $a = 0.90$  (bottom panels) in the case of counterrotating disks.

$L_{\text{Edd}} = 1.2572 \times 10^{38} (M/M_{\odot})$  erg/s are the bolometric and Eddington luminosities) and the hydrogen column density  $N_{\text{H}}$ , Liu et al. (2008, 2010) measured the spin to be  $a = 0.84 \pm 0.05$ .<sup>8</sup> The Eddington ratio is instead  $\ell = 0.0989 \pm 0.0073$  (*cf.* Table I of Liu et al. (2008) and Liu et al. (2010)). We notice that the errors on  $a$  and  $\ell$  include also the (propagated) effect of the uncertainties on  $M$ ,  $d$  and  $i$  (Liu et al. 2008, 2010).

Our simple disk model depends on three parameters,  $a$ ,  $q$  and the Eddington ratio  $\ell = L_{\text{bol}}/L_{\text{Edd}}$ . The latter can be reexpressed as  $\ell = \dot{M}/\dot{M}_{\text{Edd}}(a, q)$ , where we define the Eddington accretion rate as

$$\dot{M}_{\text{Edd}}(a, q) = \frac{L_{\text{Edd}}}{\eta(a, q)c^2}, \quad (11)$$

$\eta = 1 - E_{\text{ISCO}}(r_{\text{ISCO}})$  being the efficiency of the conversion between rest-mass and electromagnetic energy (Misner et al. 1973). Ideally we would then have to fit the observed spectrum of M33 X-7 with this 3-parameter model. However, because of the difficulties and subtleties of analyzing the real Chandra and XMM-Newton spectra and because of the simplified nature of our disk model, we resorted to a simpler approach. While a thorough analysis of the real data will be needed to determine the precise constraints on  $q$ , our simplified treatment will show that such an analysis is definitely worth being done as it would permit ruling out entire regions of the  $(a, q)$  plane.

In particular, instead of comparing our disk model with the raw data, we compare it to the spectrum of a thin disk with  $\ell^* = 0.0989$  and inclination  $i = 74.6^\circ$  around a Kerr BH with spin  $a^* = 0.84$  and mass  $M = 15.65M_{\odot}$  (these are the values measured for M33 X-7). While meaningful and reliable constraints on the parameter  $a$  and  $q$  can only be obtained by fitting the original X-ray data, we use here this simplified approach because ours is a preliminary investigation and our results are only meant as a qualitative guide for future more rigorous studies. The spectrum is calculated with the standard Novikov-Thorne model reviewed in section 3. The observational errors on the “measured” spectrum are then mimicked by using the estimated final errors on the spin ( $\delta a = 0.05$ ) and Eddington ratio ( $\delta \ell = 0.0073$ ). Because the Eddington ratio regulates the bolometric luminosity (*i.e.*, the normalization of the spectrum) one has  $L^{\text{Kerr}}(\nu, a^*, \ell^*) < L^{\text{Kerr}}(\nu, a^* \pm \delta a, \ell^* + \delta \ell)$  and  $L^{\text{Kerr}}(\nu, a^*, \ell^*) > L^{\text{Kerr}}(\nu, a^* \pm \delta a, \ell^* - \delta \ell)$ . It therefore makes sense to define the error as

$$\sigma(\nu) = \frac{\max(\nu L^{\text{Kerr}}(\nu, a^* \pm \delta a, \ell^* + \delta \ell)) - \min(\nu L^{\text{Kerr}}(\nu, a^* \pm \delta a, \ell^* - \delta \ell))}{2}. \quad (12)$$

<sup>8</sup> We warn the reader that this is the revised value reported in Liu et al. (2010), which corrects a bug in the analysis of Liu et al. (2008).

Binary System	$M/M_{\odot}$	$a$	Reference
4U 1543-47	$9.4 \pm 1.0$	$0.75 - 0.85$	Shafee et al. (2006)
GRO J1655-40	$6.30 \pm 0.27$	$0.65 - 0.75$	Shafee et al. (2006)
GRS 1915+105	$14.0 \pm 4.4$	$> 0.98$	McClintock et al. (2006)
LMC X-3	$5 - 11$	$< 0.26$	Davis et al. (2006)
M33 X-7	$15.65 \pm 1.45$	$0.84 \pm 0.05$	Liu et al. (2008, 2010)
LMC X-1	$10.91 \pm 1.41$	$0.92^{+0.05}_{-0.07}$	Gou et al. (2009)
XTE J1550-564	$9.10 \pm 0.61$	$0.34^{+0.20}_{-0.28}$	Steiner et al. (2010b)

TABLE 1  
PUBLISHED SPIN MEASUREMENTS OF STELLAR-MASS BH CANDIDATES WITH THE CONTINUUM FITTING METHOD.

To determine the values of  $a$ ,  $q$  and  $\ell$  giving the best fit, one would then have to minimize the reduced  $\chi^2$ , which we define as

$$\chi_{\text{red}}^2 = \frac{\chi^2}{N} = \frac{1}{N} \sum_{i=1}^{i=N} \left( \frac{\nu_i L^{\text{MN}}(\nu_i, a, q, \ell) - \nu_i L^{\text{Kerr}}(\nu_i, a^*, \ell^*)}{\sigma(\nu_i)} \right)^2 \quad (13)$$

where the summation is performed over  $N$  sampling frequencies  $\nu_i$  and where  $L^{\text{MN}}$  and  $L^{\text{Kerr}}$  are calculated as explained in Sections 4 and 3 respectively. To simplify the analysis, here we assume that the Eddington ratio is fixed to the measured value  $\ell^*$ , and therefore seek to minimize

$$\chi_{\text{red}}^2 = \frac{\chi^2}{N} = \frac{1}{N} \sum_{i=1}^{i=N} \left( \frac{\nu_i L^{\text{MN}}(\nu_i, a, q, \ell^*) - \nu_i L^{\text{Kerr}}(\nu_i, a^*, \ell^*)}{\sigma(\nu_i)} \right)^2. \quad (14)$$

We stress that this simplified approach makes sense because in principle the Eddington ratio can be determined independently, by integrating the luminosity over all frequencies.

Since the spectrum of M33 X-7 is well fit with an accretion disk around a Kerr BH (Liu et al. 2008, 2010), one may wonder whether a fit with an additional parameter is statistically justified. As already stressed, our viewpoint is that X-ray continuum spectra can be used to constrain the value of the anomalous quadrupole moment, precisely because of the data’s small error bars. This is, in other words, a null experiment, *i.e.* one in which we seek to measure a quantity which we expect to be zero. The measurement is therefore not one of the quantity itself, but rather a measurement of its “error bars” around its expected zero value.

In Fig. 8 we show the contour plots of  $\log_{10}(\chi_{\text{red}}^2)$ , as a function of  $a$  and  $q$  and as given by Eq. (14), in which we choose  $N = 41$  sampling frequencies  $\nu_i$  equally spaced, in logarithmic scale, from  $10^{15}$  to  $1.5 \times 10^{18}$  Hz. Also, to calculate  $L^{\text{MN}}$  and  $L^{\text{Kerr}}$  we assume  $r_{\text{out}} = 10^3 M$ , which allows us to significantly reduce the computational time needed to produce the spectra with respect to a larger outer radius. The regions of parameter space which are viable present  $\log_{10}(\chi_{\text{red}}^2) < 0$ . As expected,  $\chi_{\text{red}}^2$  presents a minimum around  $a^* = 0.84$ ,  $q = 0$  (due to Eq. (14),  $\chi_{\text{red}}^2$  is exactly 0 there), but also the surrounding “valley” is in agreement with the data (see the right panel of Fig. 8). Moreover, a larger “valley” (featuring a central “basin”) with  $\chi_{\text{red}}^2 < 1$  exists for  $q \lesssim -0.3$  and  $a \gtrsim -0.5$ , separated from the first one by a saddle.

The physical interpretation of these two allowed “valleys” is quite straightforward. They stretch across the red line in Fig. 8, which corresponds the  $(a, q)$  for which  $\eta(a, q) = \eta(a = a^*, q = 0)$ , where  $\eta(a = a^*, q = 0)$  is the efficiency of the Kerr model that we use to mimic the data for M33 X-7.<sup>9</sup> This fact is easy to understand. In our analysis we assume that the bolometric luminosity,  $L_{\text{bol}} = \eta(a, q) \dot{M} c^2$  is fixed and given by  $\ell^* L_{\text{edd}} = \eta(a = a^*, q = 0) \dot{M}^* c^2$ , where  $\dot{M}^*$  denotes the accretion rate of M33 X-7. The accretion rate  $\dot{M}$  is constrained to be close to  $\dot{M}^*$  in order for the Manko-Novikov spectrum to reproduce that of M33 X-7 at low frequencies. This is because  $\dot{M}$  basically regulates the slope of the spectrum at low frequencies: from Eq. (6) one gets  $L(\nu) \sim T$  at small frequencies, but  $T \propto \dot{M}^{1/4}$  because of Eq. (3) and the blackbody assumption. Therefore, if  $\dot{M} \sim \dot{M}^*$  one obtains that it must be  $\eta(a, q) \sim \eta(a = a^*, q = 0)$ .

We stress that we have determined these two allowed regions under the conservative assumption (12) for the error  $\sigma$ . In Eq. (12) we basically assumed that the errors determined by Liu et al. (2008, 2010) for  $\ell$  and  $a$  were uncorrelated, which could result in an estimate slightly larger than the real observational errors. This is hinted at also by Fig. 8. If one assumes  $q = 0$  (*i.e.*, if one adopts the Kerr-BH hypothesis) Fig. 8 shows that the allowed spins would be  $0.65 \lesssim a \lesssim 0.95$ , whereas Liu et al. (2008, 2010) find  $a^* = 0.84 \pm 0.05$ . If our naive assumption overestimated the real observational errors by a factor  $\sqrt{10} \approx 3.16$ ,  $\chi_{\text{red}}^2$  would decrease by a factor 10, effectively restricting the allowed  $(a, q)$  to the regions of Fig. 8 where  $\log_{10}(\chi_{\text{red}}^2) < -1$ . One can see that for  $q = 0$ ,  $\log_{10}(\chi_{\text{red}}^2) < -1$  would indeed give  $0.79 \lesssim a \lesssim 0.88$ , similar to the interval identified by Liu et al. (2008, 2010). Likewise, an observational error 10 times smaller than Eq. (12) would constrain the viable models to the regions with  $\log_{10}(\chi_{\text{red}}^2) < -2$ .

<sup>9</sup> The redline disappears for  $-0.29 \lesssim q \lesssim -0.05$  because of the discontinuous dependence of the ISCO on  $(a, q)$  (see Appendix B).

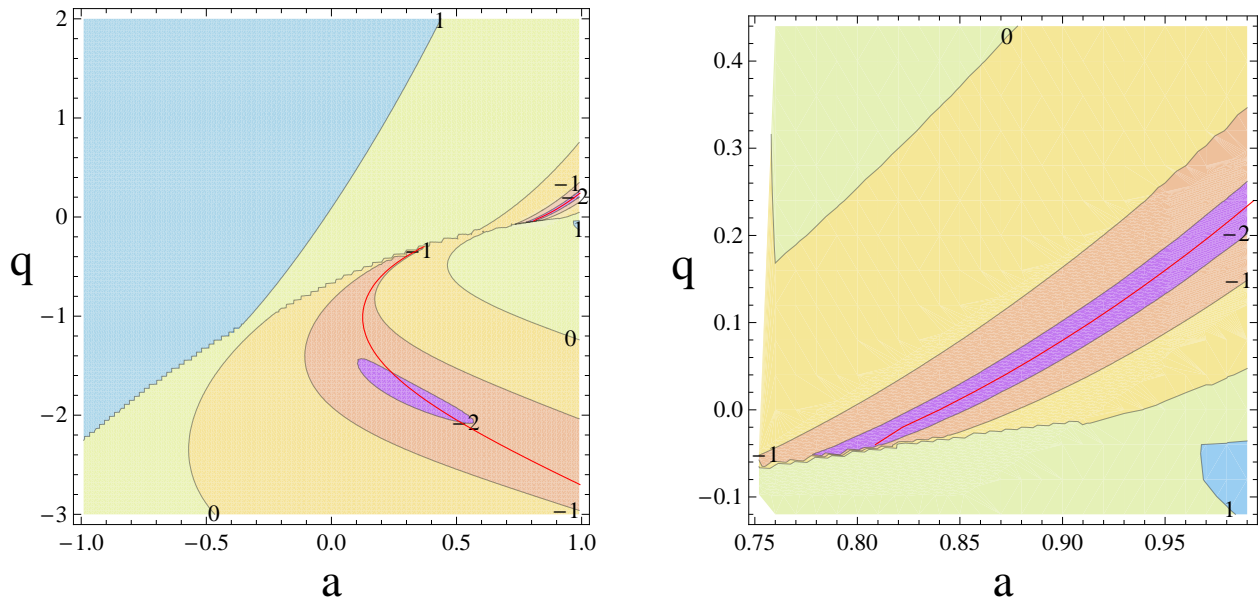


FIG. 8.—  $\log_{10}(\chi_{\text{red}}^2)$ , as defined by Eq. (14), for the comparison between the spectrum of M33 X-7 and that of a thin accretion disk in a Manko-Novikov spacetime with spin  $a$  and quadrupole parameter  $q$  (as defined in Eq. (10)). Instead of fitting the original X-ray data, we use a simplified model for the spectrum of M33 X-7 (see text for details), and therefore the constraints  $a$  and  $q$  only have a qualitative meaning. The viable regions are those with  $\log_{10}(\chi_{\text{red}}^2) < 0$ , hence ruling out roughly half of the  $(a, q)$  plane. Our naive assumption (12) for the errors probably overestimates the real observational uncertainties (see text for details). If the error (12) were too large by a factor  $\sqrt{10} \approx 3.16$  (10),  $\chi_{\text{red}}^2$  would decrease by a factor 10 (100), effectively restricting the allowed  $(a, q)$  to the regions with  $\log_{10}(\chi_{\text{red}}^2) < -1$  ( $\log_{10}(\chi_{\text{red}}^2) < -2$ ). The red line denotes the  $(a, q)$  for which the efficiency  $\eta(a, q)$  equals that of M33 X-7 (see text for a physical interpretation).

Even with our conservative assumption for the errors, however, Fig. 8 shows that more than half of the  $(a, q)$  plane is ruled out. Nevertheless, if systematic errors for M33 X-7 were larger than assumed in Liu et al. (2008, 2010), the constraints might be considerably weaker. For example, if the errors were  $\sqrt{10} \approx 3.16$  larger than our assumption, only the region with  $\log_{10}(\chi_{\text{red}}^2) > 1$  would be ruled out. We discuss possible sources of systematic error in the next section. We stress, however, that the presence of significant systematics would not only jeopardize our test of the no-hair theorem, but would represent a very serious problem also for the spin measurements with the continuum fitting technique, even if the Kerr-BH hypothesis is adopted. (This can be understood by looking at Fig. 8 for  $q = 0$ : as can be seen, the allowed interval for  $a$  grows rapidly if the error increases.)

## 6. POSSIBLE SOURCES OF SYSTEMATIC ERRORS

The continuum fitting method is a very promising technique for probing the space-time of stellar-mass BH candidates. Nevertheless, it is important to keep in mind that there are sources of systematic errors that still need to be understood in order to obtain robust estimates of the spin parameter (if one assumes the Kerr-BH hypothesis) or constraints on the anomalous quadrupole moment with this method.

The main source of uncertainty is the estimate of the hardening factor, sometimes called color factor,  $f_{\text{col}}$ . Because in the inner part of the disk the temperature exceeds  $10^6$  K, non-thermal processes are non-negligible and the spectrum observed by a distant observer is not the blackbody-like spectrum computed from the disk's effective temperature  $T$ . The hardening factor takes this effect into account, by replacing  $T$  with the color temperature  $T_{\text{col}} = f_{\text{col}}T$ , and its typical values are in the range  $f_{\text{col}} = 1.5 - 2.0$ . The computation of the hardening factor requires a reliable model of the disk atmosphere and its importance has been already stressed in Li et al. (2005). Significant progresses to address this issue have been done in Davis et al. (2005) and in Davis & Hubeny (2006).

The continuum fitting technique also assumes that the spin of the compact object is perpendicular to the inner part of the accretion disk to within a few degrees. For stellar-mass BH candidates in X-ray binary systems, we expect this to be true, on the basis of binary population synthesis (Fragos et al. 2010). While the Bardeen-Petterson effect (Bardeen & Petterson 1975) may also be responsible for this effect, for young objects the timescale necessary to align the central part of the disk turns out to be too long. However, there are also observational data (Maccarone 2002) and theoretical arguments (Fragile et al. 2001) suggesting that tilted disks may be possible. This assumption will be checked by future X-ray polarimetry observations (Li et al. 2009; Schnittman & Krolik 2009, 2010), such as the GEMS mission scheduled for 2014.

In our current analysis, we have also neglected the effect of light bending, because this is just a preliminary study to determine whether the continuum fitting method can conceivably be used to constrain deviations from the Kerr metric. While the effect of light bending must be taken into account in a complete analysis of the observational data, it has been quite commonly neglected in similar preliminary studies appeared in the literature (Harko et al. 2009a,b,

2010a,b; Kovacs & Harko 2010).

## 7. CONCLUSIONS

If current astrophysical BH candidates are Kerr BHs, their spacetime should be completely specified by two parameters, namely their mass  $M$  and spin  $J$ . This can be tested by measuring at least three multipole moments of the BH candidate. While there are several proposals to obtain such a measurement with future experiments, in this paper we have shown that current X-ray observations of stellar-mass BH candidates in binary systems can already be used to constrain possible deviations from the Kerr metric.

We have computed the thermal spectrum of a geometrically thin and optically thick accretion disk around a compact object with mass  $M$ , spin parameter  $|a| \leq 1$  and arbitrary anomalous quadrupole moment  $q$ . For  $q = 0$ , we recover the Kerr metric. The exact value of  $q$  determines the inner radius of the disk, changing the high frequency region of the spectrum. The effect is small for low spin parameters or for counterrotating disk, but it becomes important for higher values of  $a$ . In general, the sole analysis of the disk spectrum cannot completely determine  $q$ , because the spectrum is degenerate in  $a$  and  $q$  and therefore one would need an independent measure of  $a$ . However, for very fast-rotating Kerr BHs the ISCO radius and therefore the disk's inner radius becomes very small. Any deviation from  $q = 0$  (*i.e.*, from the Kerr solution) makes the inner radius grow quickly. Since current observations suggest that the inner radius of the accretion disk of some stellar-mass BH candidates is close to the gravitational radius  $R_g = GM/c^2$ , one can constrain the anomalous quadrupole moment of these objects very efficiently.

In this paper we have considered a specific example, the stellar-mass BH candidate M33 X-7, whose estimated spin is  $a = 0.84 \pm 0.05$  if one assumes it is a Kerr BH (Liu et al. 2008, 2010). Since stronger constraints on  $q$  can be obtained from objects with higher  $a$ , we could have considered GRS 1915 + 105, whose spin parameter has been estimated to be larger than 0.98 in McClintock et al. (2006) under the Kerr-BH assumption. However, the measurements of the distance, mass and viewing angle of M33 X-7 are more reliable, thus making this object more suitable to obtain preliminary constraints on the  $a - q$  plane.

To move our analysis beyond the simplified and preliminary stage we achieved in this paper, it is of paramount importance to properly understand the systematic errors that might affect the continuum fitting method, and which could in principle blur the difference between the spectra of Kerr BHs and those of other objects, and affect the measurements of the spin even if one adopts the Kerr BH hypothesis. Moreover, we will have to amend our disk model by including the following ingredients:

1. *The effect of light bending.* A rigorous computation of the spectrum requires to trace the light rays from the surface of the accretion disk to the distant observer in the background metric. The effect of light bending is presumably no less important than the other relativistic effects and further alters the observed spectrum.
2. *The spectral hardening factor.* In the inner part of the accretion disk, the temperature is high and non-blackbody effects cannot be neglected. We thus need an accurate model of the disk atmosphere for computing the spectral hardening factor (Shimura & Takahara 1995; Merloni et al. 2000; Davis et al. 2005).
3. Additional effects to be considered in an accurate study are the ones of limb darkening and of returning radiation.

We would like to thank M. C. Miller and R. Takahashi for critically reading a preliminary version of this manuscript and providing useful feedback. E.B. would like to thank J. Brink and I. Mandel for pointing out a few typos in the original Manko-Novikov metric. C.B. wishes to acknowledge the Horace Hearne Institute for Theoretical Physics at Louisiana State University and the Michigan Center for Theoretical Physics at the University of Michigan, for support and hospitality when this work was finalized. The work of C.B. was supported by World Premier International Research Center Initiative (WPI Initiative), MEXT, Japan, and by the JSPS Grant-in-Aid for Young Scientists (B) No. 22740147. E.B. acknowledges support from NSF Grants PHY-0903631, and would like to acknowledge support and hospitality from the Institute for the Physics and Mathematics of the Universe at The University of Tokyo, where this work was started.

## APPENDIX

### MANKO-NOVIKOV SPACETIMES

The Manko-Novikov metric is a stationary, axisymmetric, and asymptotically flat exact solution of the vacuum Einstein equations (Manko & Novikov 1992). It is not a BH solution<sup>10</sup>, but it can be used to describe the gravitational field outside a generic body like a compact star. The line element in quasi-cylindrical and prolate spheroidal coordinates

<sup>10</sup> The Manko-Novikov spacetimes have naked singularities and closed time-like curves exterior to a horizon. Therefore, the no-hair theorem does not apply and the solution can have an infinite number of free parameters. Let us notice, however, that all these pathological features happen at very small radii and can be neglected in our study, because they are inside the inner radius of the disk. Here the basic idea is that naked singularities and closed time-like curves do not exist in reality because they are “covered” by some exotic object, whose exterior gravitational field is described by the Manko-Novikov metric.

is respectively

$$\begin{aligned} ds^2 &= -f(dt - \omega d\phi)^2 + \frac{e^{2\gamma}}{f}(d\rho^2 + dz^2) + \frac{\rho^2}{f}d\phi^2 = \\ &= -f(dt - \omega d\phi)^2 + \frac{k^2 e^{2\gamma}}{f}(x^2 - y^2) \left( \frac{dx^2}{x^2 - 1} + \frac{dy^2}{1 - y^2} \right) + \frac{k^2}{f}(x^2 - 1)(1 - y^2)d\phi^2, \end{aligned} \quad (\text{A1})$$

where

$$f = e^{2\psi} A/B, \quad (\text{A2})$$

$$\omega = 2ke^{-2\psi} C A^{-1} - 4k\alpha(1 - \alpha^2)^{-1}, \quad (\text{A3})$$

$$e^{2\gamma} = e^{2\gamma'} A(x^2 - 1)^{-1}(1 - \alpha^2)^{-2}, \quad (\text{A4})$$

and

$$\psi = \sum_{n=1}^{+\infty} \frac{\alpha_n P_n}{R^{n+1}}, \quad (\text{A5})$$

$$\begin{aligned} \gamma' &= \frac{1}{2} \ln \frac{x^2 - 1}{x^2 - y^2} + \sum_{m,n=1}^{+\infty} \frac{(m+1)(n+1)\alpha_m \alpha_n}{(m+n+2)R^{m+n+2}} (P_{m+1}P_{n+1} - P_m P_n) + \\ &+ \left[ \sum_{n=1}^{+\infty} \alpha_n \left( (-1)^{n+1} - 1 + \sum_{k=0}^n \frac{x-y + (-1)^{n-k}(x+y)}{R^{k+1}} P_k \right) \right], \end{aligned} \quad (\text{A6})$$

$$A = (x^2 - 1)(1 + ab)^2 - (1 - y^2)(b - a)^2, \quad (\text{A7})$$

$$B = [x + 1 + (x - 1)ab]^2 + [(1 + y)a + (1 - y)b]^2, \quad (\text{A8})$$

$$C = (x^2 - 1)(1 + ab)[b - a - y(a + b)] + (1 - y^2)(b - a)[1 + ab + x(1 - ab)], \quad (\text{A9})$$

$$a = -\alpha \exp \left[ \sum_{n=1}^{+\infty} 2\alpha_n \left( 1 - \sum_{k=0}^n \frac{(x-y)}{R^{k+1}} P_k \right) \right], \quad (\text{A10})$$

$$b = \alpha \exp \left[ \sum_{n=1}^{+\infty} 2\alpha_n \left( (-1)^n + \sum_{k=0}^n \frac{(-1)^{n-k+1}(x+y)}{R^{k+1}} P_k \right) \right]. \quad (\text{A11})$$

Here  $R = \sqrt{x^2 + y^2 - 1}$  and  $P_n$  are the Legendre polynomials with argument  $xy/R$ :

$$P_n = P_n \left( \frac{xy}{R} \right), \quad P_n(x) = \frac{1}{2^n n!} \frac{d^n}{dx^n} (x^2 - 1)^n. \quad (\text{A12})$$

We notice that Eqs. (A6), (A10) and (A11) correct a few typos in the original Manko-Novikov metric written in Manko & Novikov (1992): see Brink (2008) and Fang (2007).

The solution has an infinite number of free parameters:  $k$ ,  $\alpha$ , and  $\alpha_n$  ( $n = 1, \dots, +\infty$ ). For  $\alpha \neq 0$  and  $\alpha_n = 0$ , it reduces to the Kerr metric. For  $\alpha = \alpha_n = 0$ , we find the Schwarzschild solution. For  $\alpha = 0$  and  $\alpha_n \neq 0$ , we obtain the static Weyl metric. Without loss of generality, we can put  $\alpha_1 = 0$  to bring the massive object to the origin of the coordinate system. In this paper, we have restricted our attention to the subclass of Manko-Novikov spacetimes discussed in Gair et al. (2008), where  $\alpha_n = 0$  for  $n \neq 2$ . Therefore, we have three free parameters ( $k$ ,  $\alpha$ , and  $\alpha_2$ ), which are related to the mass,  $M$ , the dimensionless spin parameter,  $a = J/M^2$ , and the dimensionless anomalous quadrupole moment,  $q = -(Q - Q_{\text{Kerr}})/M^3$ , of the object by the relations

$$\alpha = \frac{\sqrt{1 - a^2} - 1}{a}, \quad k = M \frac{1 - \alpha^2}{1 + \alpha^2}, \quad \alpha_2 = q \frac{M^3}{k^3}. \quad (\text{A13})$$

Let us notice that  $q$  measures the deviation from the quadrupole moment of a Kerr BH. In particular, since  $Q_{\text{Kerr}} = -a^2 M^3$ , the solution is oblate for  $q > -a^2$  and prolate for  $q < -a^2$ . However, when  $q \neq 0$ , even all the higher order multipole moments of the spacetime have a different value from the Kerr ones.

It is often useful to change coordinate system. The relation between the prolate spheroidal coordinates and the quasi-cylindrical coordinates is given by

$$\rho = k \sqrt{(x^2 - 1)(1 - y^2)}, \quad z = kxy, \quad (\text{A14})$$

with inverse

$$\begin{aligned} x &= \frac{1}{2k} \left( \sqrt{\rho^2 + (z+k)^2} + \sqrt{\rho^2 + (z-k)^2} \right), \\ y &= \frac{1}{2k} \left( \sqrt{\rho^2 + (z+k)^2} - \sqrt{\rho^2 + (z-k)^2} \right). \end{aligned} \quad (\text{A15})$$

The relation between the standard Schwarzschild coordinates and the quasi-cylindrical coordinates is given by

$$\rho = \sqrt{r^2 - 2Mr + a^2 M^2} \sin \theta, \quad z = (r - M) \cos \theta. \quad (\text{A16})$$

#### CIRCULAR ORBITS ON THE EQUATORIAL PLANE AND ISCO

The line element of a generic stationary and axisymmetric spacetime can be written as

$$ds^2 = g_{tt}dt^2 + 2g_{t\phi}dtd\phi + g_{rr}dr^2 + g_{zz}dz^2 + g_{\phi\phi}d\phi^2. \quad (\text{B1})$$

Since the metric is independent of the  $t$  and  $\phi$  coordinates, we have the conserved specific energy at infinity,  $E$ , and the conserved  $z$ -component of the specific angular momentum at infinity,  $L_z$ . This fact allows to write the  $t$ - and  $\phi$ -component of the 4-velocity of a test-particle as

$$u^t = \frac{Eg_{\phi\phi} + L_z g_{t\phi}}{g_{t\phi}^2 - g_{tt}g_{\phi\phi}}, \quad u^\phi = -\frac{Eg_{t\phi} + L_z g_{tt}}{g_{t\phi}^2 - g_{tt}g_{\phi\phi}}. \quad (\text{B2})$$

From the conservation of the rest-mass,  $g_{\mu\nu}u^\mu u^\nu = -1$ , we can write

$$g_{rr}\dot{r}^2 + g_{zz}\dot{z}^2 = V_{\text{eff}}(r, z), \quad (\text{B3})$$

where the effective potential  $V_{\text{eff}}$  for fixed  $E$  and  $L_z$  is given by

$$V_{\text{eff}} = \frac{E^2 g_{\phi\phi} + 2EL_z g_{t\phi} + L_z^2 g_{tt}}{g_{t\phi}^2 - g_{tt}g_{\phi\phi}} - 1. \quad (\text{B4})$$

Writing the metric in quasi-cylindrical coordinates as in (A1), one finds

$$V_{\text{eff}} = \frac{E^2}{f} - \frac{f}{\rho^2} (L_z - \omega E)^2 - 1. \quad (\text{B5})$$

Circular orbits in the equatorial plane are located at the zeros and the turning points of the effective potential:  $\dot{r} = \dot{z} = 0$ , which implies  $V_{\text{eff}} = 0$ , and  $\ddot{r} = \ddot{z} = 0$ , requiring respectively  $\partial_r V_{\text{eff}} = 0$  and  $\partial_z V_{\text{eff}} = 0$ . From these conditions, one can obtain the angular velocity,  $E$ , and  $L_z$  of the test-particle:

$$\Omega_\pm = \frac{d\phi}{dt} = \frac{-\partial_r g_{t\phi} \pm \sqrt{(\partial_r g_{t\phi})^2 - (\partial_r g_{tt})(\partial_r g_{\phi\phi})}}{\partial_r g_{\phi\phi}}, \quad (\text{B6})$$

$$E = -\frac{g_{tt} + g_{t\phi}\Omega}{\sqrt{-g_{tt} - 2g_{t\phi}\Omega - g_{\phi\phi}\Omega^2}}, \quad (\text{B7})$$

$$L_z = \frac{g_{t\phi} + g_{\phi\phi}\Omega}{\sqrt{-g_{tt} - 2g_{t\phi}\Omega - g_{\phi\phi}\Omega^2}}, \quad (\text{B8})$$

where the sign  $+$  is for corotating orbits and the sign  $-$  for counterrotating ones. The orbits are stable under small perturbations if  $\partial_r^2 V_{\text{eff}} \leq 0$  and  $\partial_z^2 V_{\text{eff}} \leq 0$ . In Kerr spacetime, the second condition is always satisfied, so one can deduce the radius of the innermost stable circular orbit (ISCO) from  $\partial_r^2 V_{\text{eff}} = 0$ . As first noticed in Gair et al. (2008), in general that is not true in Manko-Novikov spacetimes. For  $q > 0$ ,  $\partial_z^2 V_{\text{eff}}$  is always smaller than zero and one finds that the ISCO moves to larger radii as  $q$  increases. When  $q < 0$ , for any value of the spin parameter there are two critical values, say  $q_1$  and  $q_2$  with  $q_1 > q_2$ , and:

1. For  $q > q_1$ , one proceeds as in the case  $q \geq 0$  and finds the radius of the ISCO through the equation  $\partial_r^2 V_{\text{eff}} = 0$ .  $r_{\text{ISCO}}$  decreases as  $q$  decreases.
2. For  $q_2 < q < q_1$ , there are two disconnected regions with stable orbits. The standard region  $r > r_1$ , where  $r_1$  is still given by  $\partial_r^2 V_{\text{eff}} = 0$ , and an internal region  $r_3 < r < r_2$ , where  $r_2$  is once again given by  $\partial_r^2 V_{\text{eff}} = 0$  (that is, circular orbits with  $r_2 < r < r_1$  are radially unstable), while  $r_3$  is given by  $\partial_z^2 V_{\text{eff}} = 0$  (that is, circular orbits with  $r < r_3$  are vertically unstable). As  $q$  decreases,  $r_1$  decreases, while  $r_2$  and  $r_3$  increases. When  $q = q_2$ ,  $r_1 = r_2$ .
3. For  $q < q_2$ , the ISCO is at  $r_3$ , which is given by  $\partial_z^2 V_{\text{eff}} = 0$ .

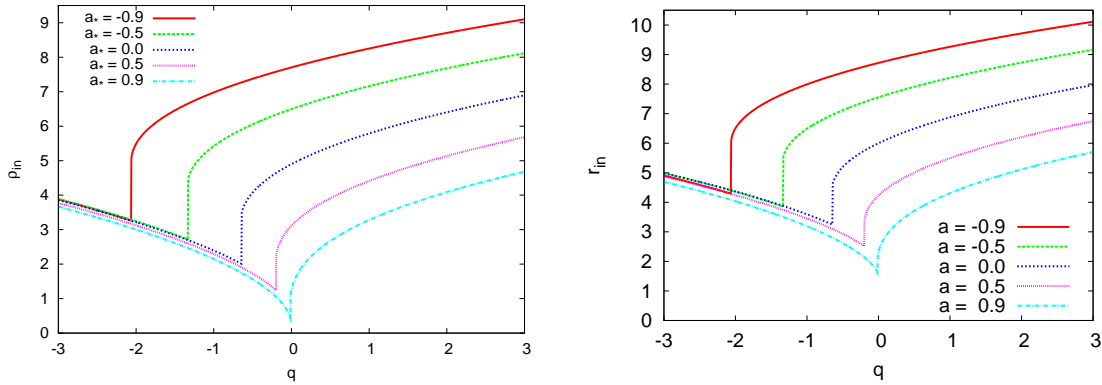


FIG. 9.— Radial coordinate of the inner radius of the disk as a function of the anomalous quadrupole moment  $q$  for different values of the spin parameter  $a$ . Left panel: radial coordinate in the quasi-cylindrical coordinates. Right panel: radial coordinate in the standard Schwarzschild coordinates. Radial coordinate in unit  $M = 1$ .

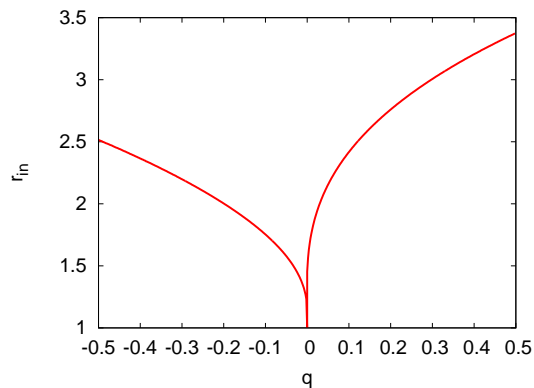


FIG. 10.— Radial coordinate in the standard Schwarzschild coordinates of the inner radius of the disk as a function of the anomalous quadrupole moment  $q$  for an extreme compact object  $a \rightarrow 1$ . Radial coordinate in unit  $M = 1$ .

For  $q > q_1$ , the inner radius of the disk is the radius of the ISCO, i.e.  $r_{\text{in}} = r_{\text{ISCO}}$ . For  $q_2 < q < q_1$ , the energy and the angular momentum of the orbits in the region  $r_3 < r < r_2$  are higher than the ones at  $r > r_1$ : the result is that the inner radius of the disk is at  $r_1$ , since the accreting matter reaches the orbit at  $r_1$ , which is a minimum of  $E$  and  $L_z$ , and then plunges to the massive object. For  $q < q_2$ , the inner radius of the disk is  $r_3$ .

In Fig. 9, we show the inner radius of the disk for a few values of the spin parameters  $a$ . In Fig. 10, we show the case of a maximally rotating object with  $a \rightarrow 1$ : it is remarkable that only in the case  $q = 0$  the inner radius of the disk goes to  $M$ . For  $q \neq 0$ , the inner radius of the disk is significantly larger. Since current observations suggest that, at least for some BH candidates, the inner radius of the disk is consistent with the one of a fast-rotating Kerr BH, deviations from the Kerr metric, if any, should not be large.

## REFERENCES

- Apostolatos, T. A., Lukes-Gerakopoulos, G., & Contopoulos, G. 2009, *Physical Review Letters*, 103, 111101
- Bambi, C., & Freese, K. 2009, *Phys. Rev. D*, 79, 043002
- Bambi, C., Freese, K., Harada, T., Takahashi, R., & Yoshida, N. 2009, *Phys. Rev. D*, 80, 104023
- Bambi, C., Harada, T., Takahashi, R., & Yoshida, N. 2010, *Phys. Rev. D*, 81, 104004
- Bambi, C., & Yoshida, N. 2010a, *Classical and Quantum Gravity*, 27, 205006
- Bambi, C., & Yoshida, N. 2010b, *Phys. Rev. D*, 82, 064002
- Bambi, C., & Yoshida, N. 2010c, *Phys. Rev. D*, 82, 124037
- Barack, L., & Cutler, C. 2007, *Phys. Rev. D*, 75, 042003
- Barausse, E., & Rezzolla, L. 2008, *Phys. Rev. D*, 77, 104027
- Barausse, E., Rezzolla, L., Petroff, D., & Ansorg, M. 2007, *Phys. Rev. D*, 75, 064026
- Barausse, E., & Sotiriou, T. P. 2008, *Physical Review Letters*, 101, 099001
- Bardeen, J. M., & Petterson, J. A. 1975, *ApJ*, 195, L65
- Berti, E. & Cardoso V. 2006, *Int. J. Mod. Phys. D15*, 2209
- Berti, E., Cardoso, V., & Starinets, A. O. 2009, *Classical and Quantum Gravity*, 26, 163001
- Brink, J. 2008, *Phys. Rev. D*, 78, 102002
- Broderick, A. E., Loeb, A., & Narayan, R. 2009, *ApJ*, 701, 1357
- Broderick, A. E., & Narayan, R. 2006, *ApJ*, 638, L21
- Carter, B. 1971, *Physical Review Letters*, 26, 331
- Chirenti, C. B. M. H., & Rezzolla, L. 2007, *Classical and Quantum Gravity*, 24, 4191
- Chirenti, C. B. M. H., & Rezzolla, L. 2008, *Phys. Rev. D*, 78, 084011
- Chruściel, P. T., & Lopes Costa, J. 2008, arXiv:0806.0016
- Collins, N. A., & Hughes, S. A. 2004, *Phys. Rev. D*, 69, 124022
- Cowley, A. P. 1992, *ARA&A*, 30, 287
- Davis, S. W., Blaes, O. M., Hubeny, I., & Turner, N. J. 2005, *ApJ*, 621, 372
- Davis, S. W., Done, C., & Blaes, O. M. 2006, *ApJ*, 647, 525
- Davis, S. W., & Hubeny, I. 2006, *ApJS*, 164, 530
- Fang, H. 2007, Ph.D. thesis, California Institute of Technology.

- Fragile, P. C., Mathews, G. J., & Wilson, J. R. 2001, *ApJ*, 553, 955
- Fragos, T., Tremmel, M., Rantsiou, E., & Belczynski, K. 2010, *ApJ*, 719, L79
- Gair, J. R., Li, C., & Mandel, I. 2008, *Phys. Rev. D*, 77, 024035
- Glampedakis, K., & Babak, S. 2006, *Classical and Quantum Gravity*, 23, 4167
- Geroch, R. 1970, *J. Math. Phys.*, 11, 2580
- Gou, L., et al. 2009, *ApJ*, 701, 1076
- Hansen, R. 1974 *J. Math. Phys.*, 15, 46
- Harko, T., Kovács, Z., & Lobo, F. S. N. 2009a, *Classical and Quantum Gravity*, 26, 215006
- Harko, T., Kovács, Z., & Lobo, F. S. N. 2009b, *Phys. Rev. D*, 79, 064001
- Harko, T., Kovács, Z., & Lobo, F. S. N. 2010a, arXiv:1009.1958
- Harko, T., Kovács, Z., & Lobo, F. S. N. 2010b, *Classical and Quantum Gravity*, 27, 105010
- Hughes, S. A. 2006, arXiv:gr-qc/0608140
- Johannsen, T., & Psaltis, D. 2010a, *ApJ*, 716, 187
- Johannsen, T., & Psaltis, D. 2010b, *ApJ*, 718, 446
- Johannsen, T., & Psaltis, D. 2010c, arXiv:1010.1000
- Kalogera, V., & Baym, G. 1996, *ApJ*, 470, L61
- Kerr, R. P. 1963, *Phys. Rev. Lett.*, 11, 237
- Kesden, M., Gair, J., & Kamionkowski, M. 2005, *Phys. Rev. D*, 71, 044015
- Kodama, H., & Hikida, W. 2003, *Classical and Quantum Gravity*, 20, 5121
- Kormendy, J., & Richstone, D. 1995, *ARA&A*, 33, 581
- Kovacs, Z., & Harko, T. 2010, arXiv:1011.4127
- Li, L.-X., Narayan, R., & McClintock, J. E. 2009, *ApJ*, 691, 847
- Li, L.-X., Zimmerman, E. R., Narayan, R., & McClintock, J. E. 2005, *ApJS*, 157, 335
- Liang, E. P. 1998, *Phys. Rep.*, 302, 67
- Liu, J., McClintock, J. E., Narayan, R., Davis, S. W., & Orosz, J. A. 2008, *ApJ*, 679, L37
- Liu, J., McClintock, J. E., Narayan, R., Davis, S. W., & Orosz, J. A. 2010, *ApJ*, 719, L109
- Lukes-Gerakopoulos, G., Apostolatos, T. A., & Contopoulos, G. 2010, *Phys. Rev. D*, 81, 124005
- Maccarone, T. J. 2002, *MNRAS*, 336, 1371
- Manko, V. S., & Moreno, C. 1997, *Modern Physics Letters A*, 12, 613
- Manko, V. S., & Novikov, I. D. 1992, *Classical and Quantum Gravity*, 9, 2477
- Maoz, E. 1998, *ApJ*, 494, L181
- Mazur, P. O. & Mottola, E. 2004, *Proc. Nat. Acad. Sci.* 111, 9545
- McClintock, J. E., Narayan, R., Gou, L., Liu, J., Penna, R. F., & Steiner, J. F. 2010, *American Institute of Physics Conference Series*, 1248, 101
- McClintock, J. E., Shafee, R., Narayan, R., Remillard, R. A., Davis, S. W., & Li, L.-X. 2006, *ApJ*, 652, 518
- Merloni, A., Fabian, A. C., & Ross, R. R. 2000, *MNRAS*, 313, 193
- Merritt, D., Alexander, T., Mikkola, S., & Will, C. M. 2010, *Phys. Rev. D*, 81, 062002
- Miller, M. C., & Colbert, E. J. M. 2004, *International Journal of Modern Physics D*, 13, 1
- Misner, C. W., Thorne, K. S., & Wheeler, J. A. 1973, *San Francisco: W.H. Freeman and Co.*, 1973,
- Noble, S. C., Krolik, J. H., & Hawley, J. F. 2010, *ApJ*, 711, 959
- Novikov, I. D., & Thorne, K. S. 1973, in *Black Holes*, edited by C. De Witt and B. De Witt (Gordon and Breach, New York, US), 343
- Orosz, J. A., et al. 2007, *Nature*, 449, 872
- Page, D. N., & Thorne, K. S. 1974, *ApJ*, 191, 499
- Pani, P., Barausse, E., Berti, E., & Cardoso, V. 2010, *Phys. Rev. D*, 82, 044009
- Penna, R. F., McKinney, J. C., Narayan, R., Tchekhovskoy, A., Shafee, R., & McClintock, J. E. 2010, *MNRAS*, 408, 752
- Pietsch, W., Haberl, F., Sasaki, M., Gaetz, T. J., Plucinsky, P. P., Ghavamian, P., Long, K. S., & Pannuti, T. G. 2006, *ApJ*, 646, 420
- Psaltis, D., & Johannsen, T. 2010, arXiv:1011.4078
- Remillard, R. A., & McClintock, J. E. 2006, *ARA&A*, 44, 49
- Rhoades, C. E., & Ruffini, R. 1974, *Physical Review Letters*, 32, 324
- Robinson, D. C. 1975, *Physical Review Letters*, 34, 905
- Ryan, F. D. 1995, *Phys. Rev. D*, 52, 5707
- Ryan, F. D. 1997a, *Phys. Rev. D*, 56, 1845
- Ryan, F. D. 1997b, *Phys. Rev. D*, 56, 7732
- Schnittman, J. D., & Krolik, J. H. 2009, *ApJ*, 701, 1175
- Schnittman, J. D., & Krolik, J. H. 2010, *ApJ*, 712, 908
- Shafee, R., McClintock, J. E., Narayan, R., Davis, S. W., Li, L.-X., & Remillard, R. A. 2006, *ApJ*, 636, L113
- Shafee, R., Narayan, R., & McClintock, J. E. 2008, *ApJ*, 676, 549
- Shimura, T., & Takahara, F. 1995, *ApJ*, 445, 780
- Schödel, R., et al. 2002, *Nature*, 419, 694
- Sopuerta, C. F., & Yunes, N. 2009, *Phys. Rev. D*, 80, 064006
- Steiner, J. F., McClintock, J. E., Remillard, R. A., Gou, L., Yamada, S., & Narayan, R. 2010a, *ApJ*, 718, L117
- Steiner, J. F., et al. 2010b, arXiv:1010.1013
- Takahashi, R., & Harada, T. 2010, *Classical and Quantum Gravity*, 27, 075003
- Titarchuk, L., Laurent, P., & Shaposhnikov, N. 2009, *ApJ*, 700, 1831
- Tomimatsu, A., & Sato, H. 1972, *Physical Review Letters*, 29, 1344
- Torres, D. F., Capozziello, S., & Lambiase, G. 2000, *Phys. Rev. D*, 62, 104012
- Tsiklauri, D., & Viollier, R. D. 1998, *ApJ*, 500, 591
- Vigeland, S. J., & Hughes, S. A. 2010, *Phys. Rev. D*, 81, 024030
- Wex, N., & Kopeikin, S. M. 1999, *ApJ*, 514, 388
- Will, C. M. 2008, *ApJ*, 674, L25
- Zhang, S. N., Cui, W., & Chen, W. 1997, *ApJ*, 482, L155